

JPL D-13945

# LightSAR Science Requirements and Mission Enhancements

Report of the LightSAR Science Working Group (LSWG)

**Diane L. Evans**

**Mahta Moghaddam**

**Editors**

**March 1998**



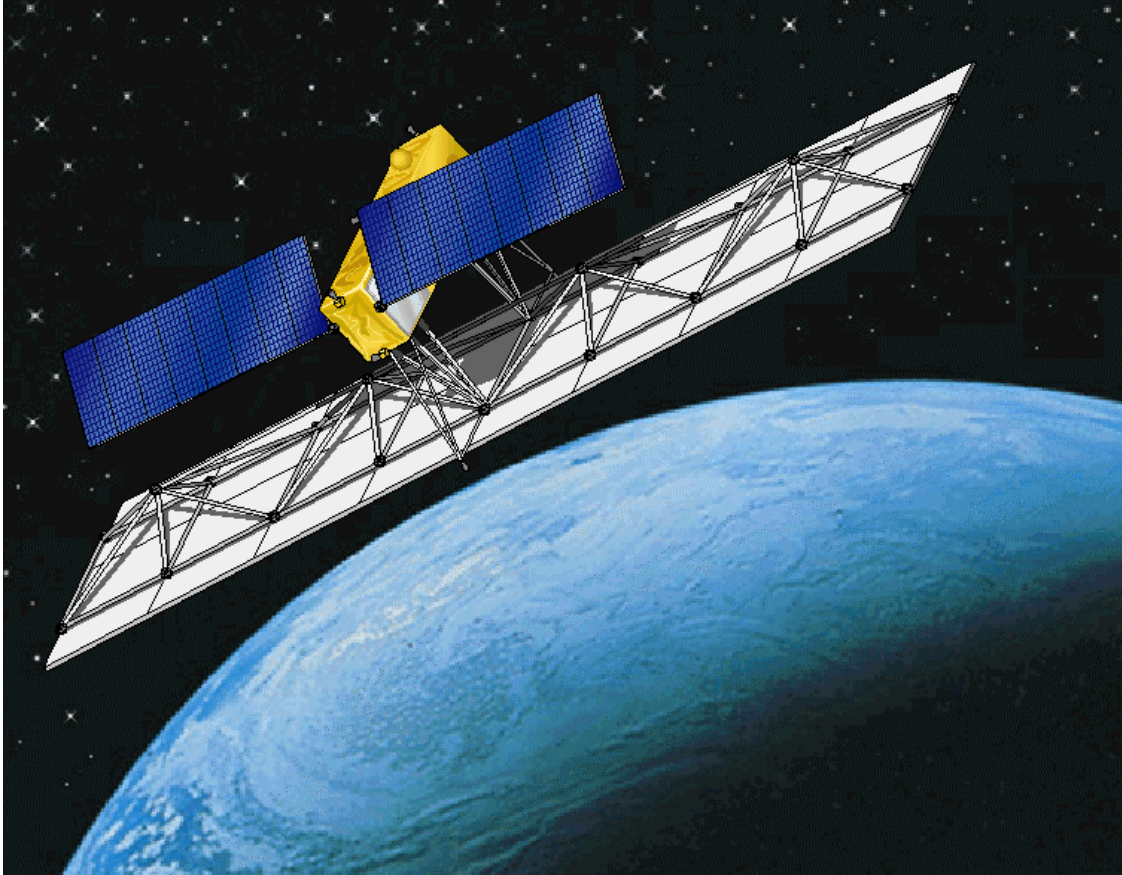
National Aeronautics and  
Space Administration

**Jet Propulsion Laboratory**  
California Institute of Technology  
Pasadena California

**Table of Contents**

**1. Introduction**..... 1  
     1.1 Background..... 1  
**2. Science Objectives**..... 2  
     2.1 Natural Hazards ..... 2  
     2.2 Ice Sheet Mass Balance and Sea Level ..... 4  
     2.3 The Carbon Cycle ..... 6  
     2.4 The Hydrologic Cycle ..... 8  
     2.5 The Role of the Ocean in Climate Change..... 10  
**3. LightSAR Sensor Requirements**..... 12  
     3.1 Frequency ..... 12  
     3.2 Change Detection..... 12  
     3.3 Multi-incidence-angle Observations..... 12  
     3.4 Polarimetric Observations..... 12  
     3.5 Wide-swath/Dual-polarization Mode..... 12  
**4. LightSAR Orbital Requirements**..... 13  
     4.1 Inclination ..... 13  
     4.2 Repeat / Revisit Period..... 13  
     4.3 Orbital Control ..... 13  
     4.4 Orbital Knowledge..... 13  
**5. LightSAR Operational Requirements**..... 13  
     5.1 Mission Duration ..... 13  
     5.2 Data Volume and Rate ..... 13  
     5.3 Real-time Mission Planning..... 14  
**6. Mode-specific Requirements**..... 14  
     6.1 Radiometric Accuracy and Precision ..... 14  
     6.2 Phase Accuracy and Precision ..... 14  
     6.3 Channel-to-channel Amplitude Calibration ..... 14  
     6.4 Polarization Isolation ..... 14  
     6.5 Noise-equivalent  $S_0$  ..... 14  
**7. Recommended Mission Enhancements**..... 15  
     7.1 Direct-broadcast Capability..... 15  
     7.2 Added Frequency (C or X Band)..... 15  
**8. Acknowledgement**..... 15  
 Figure 1. Flow from Science Objectives to Requirements ..... 16  
 Figure 2. Sample Coverage Requirements for Interferometry ..... 17  
 Table 1. Current and Planned SAR systems ..... 18  
 Table 2. Examples of SAR Applications ..... 19  
 Appendix A. LightSAR Science Working Group (LSWG) Members..... 20  
 Appendix B. Additional Science Contacts..... 21  
 Appendix C. References ..... 22

# LightSAR Science Requirements



## 1. Introduction

This document reports the recommendations of the LightSAR Science Working Group (LSWG). The LSWG was appointed by NASA in 1997 to advise on science applications for a high-technology, low-cost, Earth-imaging, Lightweight Synthetic Aperture Radar (LightSAR) satellite mission. LSWG membership is shown in Appendix A. Additional science contacts at JPL are listed in Appendix B.

The task of the LSWG was to select the measurements that could best be addressed by SAR data and that offered the highest science payoff. This task was guided by the goals of NASA's Earth Science Enterprise (ESE), formerly referred to as Mission to Planet Earth (see "Strategic Enterprise Plan 1996-2002," MTPE, HQ, NASA, March 1996). ESE relevance and scientific need had to be balanced against cost and complexity. Other factors to be considered were the current and future availability of SAR data from other sources (Table 1), the uniqueness of the SAR measurements relative to other sensor types, and the maturity of the derived data products.

The LightSAR science requirements identified in this document would satisfy the needs of a significant segment of the science community. A spaceborne SAR platform as recommended by the LSWG can supply valuable information in a broad range of Earth science disciplines. Unfortunately, a low-cost, reduced-capability SAR cannot satisfy all of them.

The LSWG finds that the higher-priority science objectives are those that can be accomplished by repeat-pass interferometry with a single polarization—i.e., L-band (24 cm wavelength) SAR. These objectives include seismic and volcanic deformation mapping, vector ice sheet and glacier velocity mapping, topographic mapping, and surface characterization. These objectives are integral to the Solid Earth & Natural Hazards discipline of the ESE strategic plan priorities. The LSWG also finds that the other high-priority science objectives—namely, the study of Earth's carbon and hydrologic cycles—are best studied by L-band polarimetric SAR. Specific objectives to be met here include monitoring forest regrowth, estimating soil moisture, and estimating snow density. These objectives address the Land Cover/Land Use Change, Short-term Climate Change, and Seasonal-to-Interannual Climate Change disciplines of the ESE strategic plan priority areas. Finally, oceanographic applications require a wide-swath mode (250-500 km) and would also benefit from dual polarization capabilities (HH and VV). These applications would address the Seasonal-to-Interannual Climate Change discipline of the ESE strategic plan. All of the above science objectives are best addressed by LightSAR data, and they all have broad multidisciplinary community support.

### 1.1 Background

SAR data provide unique information about Earth's surface and biodiversity, including critical data on natural hazards and data for use in resource assessments. SAR interferometric capabilities, which allow measurement of large-scale surface change at fine resolution, are required for monitoring surface topographic change and glacier ice velocity and, in many instances, for generating critical topographic data sets. Many recent literature citations have

## LightSAR Science Requirements

documented the contributions of interferometric radar to studies of earthquake mechanisms and propagation, volcanological hazard assessment, and refined measurements of the global ice-sheet mass balance, upon which an understanding of climate change depend. These interferometric observations form the core operational priorities of LightSAR.

Analysis of data from the Spaceborne Imaging Radar and X-band Synthetic Aperture Radar (SIR-C/X-SAR) indicates that multiparameter (wavelength and polarization) SAR data can provide accurate land cover classification and forest growth estimates; biomass estimation; mapping of wetlands; measurements of snow density, soil moisture, and surface roughness; characterization of oil slicks; and monitoring of sea ice thickness. While optimal frequencies and polarizations for these measurements depend on the specific application and, in some cases, environmental conditions, the more limited multiparameter data set provided by LightSAR will nonetheless contribute to research in this area. Examples of results published to date are summarized below (also see Appendix C). Assessments of the maturity of algorithms for deriving geophysical parameters from SAR data are given in Table 2.

For interferometric SAR observations it is necessary to optimize the wavelength of operation against temporal decorrelation, instrument sensitivity, and radar brightness for many surface terrains. With years of European Remote-sensing Satellite (ERS) and Japanese Earth Resources Satellite (JERS) SAR data acquired, volumes of multi-frequency, multi-polarization SIR-C/X-SAR data analyzed, and the prospect of new advances from the multi-mode Radarsat observations, it has become clear that the longer wavelengths such as L band are best suited to our identified repeat pass interferometry threshold science measurements, where the radar return is relatively insensitive to local changes on the surface. Reduction of SIR-C/X-SAR data show that this wavelength is also a good choice in polarimetric consideration. L-Band multi-temporal and multi-polarization measurements best provide capabilities to monitor changes in (1) biomass due to forest regeneration, (2) soil moisture levels, and (3) snow density. Thus, the fundamental functional requirements for LightSAR specify L band as the primary choice of frequency to meet the LightSAR science objectives.

## 2. Science Objectives

The science objectives for the LightSAR mission are grouped into a broad range of scientific disciplines. These groups are by no means all-encompassing but represent specific areas where there is an immediate and obvious need for data. These disciplines are listed below in approximate priority order according to the principles discussed above.

### 2.1 *Natural Hazards*

Over the past two decades, space geodetic techniques, in particular the Global Positioning System (GPS), have proven to be powerful tools for studying movements and deformations of the surface of the Earth and have led to major advances in understanding. But these measurements lack spatial continuity and require field equipment at each study site. Recent technological advances in spaceborne radar interferometry permit observation of millimeter-level surface deformation at 25-m resolution with worldwide accessibility. Derivation of the first

## LightSAR Science Requirements

differential interferometric maps of the co-seismic displacement of the June 28, 1992 Landers earthquake was arguably the most exciting recent result in earthquake geodesy. Nevertheless, at the present time, civilian spaceborne differential interferometry remains primarily a demonstration tool, because no mission dedicated to that purpose exists. The high-priority science goals of LightSAR are: (1) to refine our understanding of the earthquake cycle through mm-level interseismic and co-seismic vector deformation maps along faults and plate boundaries; (2) to monitor volcanoes for new activity and potential eruptions through mm-level deformation maps; and (3) to support additional natural hazards research using SAR as a rapid and weather-independent monitoring tool.

### 2.1.1 Crustal Deformation

The most challenging science goal for LightSAR is mapping slow Earth deformations. This includes the interseismic accumulation of strain leading up to earthquakes, as well as transient post-seismic strain relaxation following earthquakes. The main issue is that such signals are subtle, with mm-sized displacements and long wavelengths vulnerable to systematic measurement errors. The accumulation of strain in the Earth's crust is the first order indicator of future seismic hazard. The mission should allow for repeated measurement of surface change in seismically active areas along all continental margins, and it should provide worldwide accessibility to allow targeting of new and previously unidentified areas for study. Temporal coverage should support an interval of 8 days for any particular area, or 24 days for all areas. We also require a surface displacement resolution of 2-5 mm statistical height error to track and model wide-area deformation during and between major earthquakes. Specific high-priority zones should be imaged every orbit if possible, while other areas can be imaged no fewer than four times per year (see coverage/frequency map, Figure 2). The imaging must be accomplished from ascending and descending tracks, and looking to the right and left on orbit, in order to construct vector deformation fields.

### 2.1.2 Volcanic Hazards

The major observations in volcanology to be obtained by LightSAR are: (1) the spatial and temporal extent of deformation preceding and accompanying eruptions, which are key observables constraining models of magma migration; and (2) the spatial extent of new material produced during an eruption, derived from image decorrelation, which is an important diagnostic of the eruption process. As in earthquake studies, the mission should allow the measurement of surface change in volcanically active areas on an interval of 8 days for any particular area, or 24 days for all areas, with a surface displacement resolution of 1-3 cm statistical height error in order to track and model ground deformation prior to, during, and after volcanic eruptions or intrusive events. Surface change caused either by the emplacement of new lava flows or by the collapse of volcanic craters should also be studied via the decorrelation of radar phase information at a spatial resolution of ~25 m/pixel. Specific high-priority volcanoes (e.g., those in eruption or experiencing a "volcanic crisis" prior to eruption) must be imaged as often as possible (every orbit), while other areas should be imaged no fewer than four times per year (see coverage/frequency map). The imaging must be accomplished from ascending and descending tracks and looking to the right and left on orbit, in order to construct vector deformation fields and to provide the greatest temporal resolution of time-varying events.

## LightSAR Science Requirements

### 2.1.3 Other Hazards

LightSAR data will also be used to study a number of other natural hazards. Since floods build with time, frequent revisitation and weather-independent images will be used to plan for flood mitigation. Post-flood images will be used for quantitative damage assessment, and may be useful for rapid assessment during the immediate post-flood period when the area may still be cloud covered from continuing storms. For the same reason, SAR images may also be useful for rapid damage assessment after major hurricanes, when cloud cover and damaged infrastructure (telephones, roads, bridges) make conventional surveys difficult. Correlation measurements of landslide-prone areas will be used to detect early signs of incipient ground failure and to help assess the size and destructive potential of such events. Documenting the evolution of the correlation signatures will provide insight for physical modelling of the disasters and for formulation of mitigation strategies. LightSAR will also measure surface change caused by human activity, such as subsidence due to fluid withdrawal from aquifers or hydrocarbon reservoirs. Requirements for meeting these objectives are included in those presented in the previous two sections.

## 2.2 *Ice Sheet Mass Balance and Sea Level*

Sustained development of coastal areas worldwide has made the global economy extremely vulnerable to changes in sea level. Ice sheets and glaciers contain a frozen reservoir totaling nearly 80% of the world's fresh water and are the primary source of future sea level rise. While the general retreat of mountain glaciers globally is believed to be responsible for approximately one quarter to one third of the current 2 mm/year increase in sea level, the majority of the remainder remains unidentified. However, it is likely the result of yet-undiscovered imbalances in the large polar ice sheets. Accordingly, the role of ice sheets and glaciers in the global water cycle, especially their impact on future sea level, is a critical goal in the Long-term Climate area of the ESE Science Research Plan.

There are three specific measurements that LightSAR will be able to make that will contribute significantly to this goal. The first two, glacier and ice sheet velocities and topography are direct products of the interferometric capability of LightSAR. The third, monitoring of critical margins of ice sheets and glaciers, utilizes single-polarization amplitude SAR data. With the exception of the now-concluded ERS-1/2 tandem mission, there are no current or planned SAR interferometric missions to provide the first two types of measurements, and except for the upcoming Radarsat Antarctic Mapping Project (RAMP), lasting only 18 days, there is no SAR satellite designed to view the vast majority of Antarctica, where over 90% of the Earth's ice reservoir exists.

### 2.2.1 Glacier and Ice Sheet Velocities

Ice velocity is the fundamental parameter representing the dynamics of ice. It can be compared with "balance" velocities (determined from areal integration of the snow accumulation) to assess the state of equilibrium of any ice mass or portion of an ice mass. Even in the absence of accumulation data, the magnitude and direction of ice flow is critical input to dynamic models of

## LightSAR Science Requirements

ice flow and, when compared with surface topography, can identify regions that are far from being in equilibrium.

The mission should allow interferometric measurements from ascending and descending passes and from both north and south viewing directions to provide the full velocity vector over the greatest portion of the ice sheets possible. The mission should allow for surface deformation measurements to be processed as rapidly as possible consistent with constraints imposed by other science objectives such as coverage and signal-to-noise ratio (SNR). The longest allowable repeat interval for ice objectives is 8 days.

L-band interferometry has been successfully demonstrated on glaciers with SIR-C, but not over the drier snow on ice sheets. In terms of the expected sensitivity to ice displacement, an 8-day repeat cycle at L band compares with a 2-day repeat cycle at C band. Thus, displacements will be twice what has already been measured with the highly productive 1-day ERS-1/2 tandem data set. Based on the experience with tandem data, longer repeat periods will limit the ice areas over which displacements can be measured due to phase unwrapping difficulties. The accuracy of the LightSAR interferometric motion products will be better than 1 m/year and complementary to Global Positioning System (GPS) measurements, which will help determine the final velocity fields. It is estimated that a global coverage of ice velocity would require about 150 hours of SAR data, preferably from early fall to late spring, and that it should be undertaken once every other year. Only 90 hours of coverage would be required for these subsequent mappings, with an additional 10 hours in the even years to monitor variable glacier behavior.

### 2.2.2 Ice Surface Topography

The second interferometric product of ice sheets and glaciers is surface topography. Surface topography determines the magnitude and direction of the gravitational force driving the ice flow. Thus, the detailed shape of an ice sheet determines the boundaries of individual drainage basins contained within the ice sheet. In addition, the undulated character of the ice sheet surface provides proxy evidence of whether the ice flow is sliding over a well-lubricated bed or is frozen to the subglacial bed. Finally, the complete elevation field can be an invaluable aid to the interpolation of laser altimetry (e.g., EOS GLAS) which inherently only measures elevations along very narrow corridors across the ice sheet.

With repeat-pass interferometry, surface topography and ice velocity are both contained in any single interferogram. However, because the displacement due to surface topography is fixed in time, while motion displacements accrue, sequential interferograms can separate these two essential data sets by a technique known as double differencing. Interferometric data for double differencing and averaging would require about eight complete mappings the first year with less data in remaining years as specified in Section 2.2.1 above.

### 2.2.3 Ice Sheet and Glacier Boundaries

This is the most direct approach to detecting change but the most challenging in terms of deducing the cause of that change, given the delayed response character of slow-moving ice. Nevertheless, SAR offers the advantage of viewing through clouds, which are frequently

persistent at the edges of ice sheets and in mountainous terrain. By regularly imaging (once every 3-5 years) the Greenland and Antarctic Ice Sheets, LightSAR can contribute to building an unprecedented series of snapshots documenting the short-term evolution of these ice sheets. This objective is particularly germane given the recent and unexpected disintegration of large portions of ice shelves in the Antarctic Peninsula. Planimetric accuracies required for the intercomparison are about 100 m. Twenty-five-meter resolution imaging with a SAR instrument would require about 30 hours of data distributed over a 30-day window once every 2 years. This more modest data requirement is fulfilled by the collection of the interferometric data sets specified in Sections 2.2.1 and 2.2.2 above.

### **2.3 *The Carbon Cycle***

The global carbon cycle, especially as it relates to CO<sub>2</sub> and its important role as a greenhouse gas, is fundamental to the study of Earth's climate. SAR has contributed to this include by enhancing our abilities to (1) quantify the current rates of exchange of carbon dioxide between the atmosphere and the oceanic and terrestrial sources/sinks of carbon, (2) understand how changes in climate and the concentration of carbon dioxide will influence patterns of vegetation distribution and regrowth after disturbance, and (3) estimate how changes in climate will influence processes controlling patterns of carbon storage in terrestrial ecosystems, particularly in organic soils in high northern latitudes. While much previous work has focused on remote-sensing systems operating in the visible and near-infrared regions of the electromagnetic spectrum (e.g., MODIS, Landsat), research has also demonstrated that imaging radar systems provide useful information as well.

Notwithstanding the burning of fossil fuels, worldwide deforestation and afforestation practices are believed to have the highest impact on the net flux of greenhouse gases. Growing forests remove atmospheric CO<sub>2</sub> and sequester carbon in new or growing trees. The sequestration rate of carbon (biomass production) in tropical forests, for instance, could be as much as 10 to 20 tons/hectare per year. Natural disturbances to forests (such as fires, insects, and diseases) that result in large-scale mortality release large amounts of carbon to the atmosphere. Anthropogenic activities (such as deforestation and afforestation) also strongly influence the atmospheric carbon budget.

Since carbon is stored in the form of biomass in forests and this biomass is interdependent with factors such as nutrient fluxes, water availability, forest age, and temperature, monitoring the changes in biomass provides a critical piece of information to help us understand the global carbon cycle. Monitoring the other factors just mentioned is also important, to the extent that they influence the biomass variations. Balancing the carbon budget is still an unresolved issue. The biogeochemical cycles that determine the atmospheric concentrations of greenhouse gases are not yet completely understood. As we seek to provide a definitive answer to the global change question, our knowledge of land-atmosphere exchange at both the regional and global levels suffers from a lack of long-term observations of biomass. Among remote-sensing instruments, radar has been shown to have the unique abilities to respond to biomass over a usable range and give reliable temporal information, since it sees through cloud cover. For an L-band radar, biomass values of up to 150-200 tons/hectare have been successfully retrieved.

## LightSAR Science Requirements

### 2.3.1 Forest Regrowth and Biomass

Land cover change is one of the fundamental factors perturbing the global carbon cycle. In the most recent IPCC assessment, conversion of forests to managed systems (pastures and croplands) in the tropics was estimated to release  $1.6 (\pm)$  G<sub>t</sub>C/y to the atmosphere. Conversely, the regrowth of the mid-latitude forests harvested a half-century ago may be absorbing 0.5 to 1.0 G<sub>t</sub>C/y. In addition to identifying primary land conversion, successful efforts are underway using SAR to estimate regrowth in secondary forests, a key factor in carbon balances.

The SIR-C mission has demonstrated that a polarimetric L-band radar would enable monitoring patterns of forest regrowth following disturbance in many different forest ecosystems. The development of LightSAR, therefore, would enable ESE scientists to develop operational approaches for addressing issues (1) and (2) above. To clearly separate areas of disturbance from undisturbed areas and to produce the requisite accuracies in areal extent, a resolution of 25 meters is required. The mission should allow the measurement of forest regeneration in the worldwide belts of tropical, temperate, and boreal forest at yearly intervals over at least a 3-year period. Each region should be imaged at the same time of year: high summer for the boreal and tropical forests and the dry season(s) for the tropics. Imaging should be completed within a period of less than one month to ensure that the resulting regional maps of forest regeneration are consistent. Areas should be imaged at the same time of day in order to minimize measurement uncertainties due to the diurnal cycle. The imaging can be accomplished from either ascending or descending tracks, and looking to the right and left on orbit, in order to minimize the time taken to construct a regional image map. Look angles should be between 25° and 35°. Imaging the world's tropical and boreal forests as specified here would require a total of 72 million square kilometers or 54 hours of data every year, roughly half of which would be collected between May and July and the rest between October and December. This would require a peak rate of 1.1 minute of data per orbit during those periods.

For successful monitoring of changes in forest regeneration, results from the SIR-C mission have shown that the following things are required: a radiometric calibration uncertainty of less than 1 dB, a channel-to-channel radiometric uncertainty of less than 0.5 dB, a channel-to-channel phase uncertainty of less than 10°, a polarization purity (or isolation) of -25 dB, and a noise-equivalent sigma-naught (in all four polarimetric channels) of less than -30 dB.

### 2.4 *The Hydrologic Cycle*

The redistribution of solar energy over the globe is central to climate studies. Water plays a fundamental role in this redistribution through the energy associated with evapotranspiration, the transport of atmospheric water vapor, and precipitation. Residence time for atmospheric water is on the order of a week, and for soil moisture it ranges from a couple of days to months, which emphasizes the active nature of the hydrologic cycle.

Perhaps the most important role that the land surface plays in global circulation is the partitioning of incoming radiation into sensible and latent heat fluxes. The major factor involved in

## LightSAR Science Requirements

determining the relative proportions of the two heat fluxes is the availability of water, generally in the form of soil moisture. The role of soil moisture is equally important at smaller scales. Recent studies with mesoscale atmospheric models have similarly demonstrated a sensitivity to spatial gradients in soil moisture.

### 2.4.1 Soil Moisture

Soil moisture is an environmental descriptor that integrates much of the land surface hydrology and is the interface for interaction between the solid Earth surface and life. As central as this seems to the human existence and biogeochemical cycles, it is a descriptor that has not had widespread application as a variable in land process models. There are two primary reasons for this. First, while it can be measured at one point in time, it is a difficult variable to measure on a consistent and spatially comprehensive basis. Secondly, it exhibits very large spatial and temporal variability; thus, point measurements have very little meaning. The practical result of this is that soil moisture has not been used as a variable in any of our current hydrologic, climatic, agricultural, or biogeochemical models.

Over the past decade or so, much research into the use of remote sensing to measure soil moisture has taken place. It is generally accepted that the only way to measure soil moisture to a depth exceeding a few centimeters is with a microwave instrument operating at L band or lower frequencies. Passive microwave measurements from low-flying aircraft have proven measurement accuracies on the order of 3% volumetric soil moisture at spatial scales of a few tens of meters. Unfortunately, similar instruments operating in space require large antennas, presenting a significant technological challenge. Even if this technological challenge could be overcome, the resolution of these instruments would be limited to tens of kilometers. Given the large spatial variability of soil moisture and land cover over spatial scales much smaller than tens of kilometers, it is unclear how the resulting measurement would relate to the soil moisture at any given point inside such a large pixel.

Active microwave instruments provide an alternative way of measuring soil moisture. To estimate soil moisture from active microwave measurements, one has to separate the effects of surface roughness and soil moisture, making this generally a more challenging problem than the passive microwave case. However, several algorithms have been developed, ranging from empirical models to ones based on complex electromagnetic scattering theories. All of these algorithms seem to give similar results, with proven accuracies (when compared with *in situ* measurements) on the order of 4% volumetric soil moisture at spatial scales of a few tens of meters. Furthermore, at least one of these algorithms has been applied to SIR-C data over the Washita site in Oklahoma, and the accuracy was verified using ground-truth data.

NASA/MTPE-sponsored research using the ERS SAR has demonstrated that spaceborne SAR systems can be used to monitor relative changes in soil moisture in fire-disturbed boreal forests. In these biomes, soil moisture is a key parameter in the estimation of rates of soil respiration. It has been estimated that climate warming will result in significant increases in soil respiration and release of carbon to the atmosphere in these biomes. Thus, the ability to monitor variations in soil moisture is essential for estimating future fluxes of carbon. Polarimetric capabilities are required in order to separate the effects of changes in soil moisture from changes in biomass and

## LightSAR Science Requirements

surface roughness. This will significantly improve models of soil respiration in the boreal region.

The development of an instrument such as LightSAR would provide an invaluable opportunity to move the measurement of soil moisture from the experimental to the operational phase and to continue to extend the current algorithms to include areas with vegetation exceeding Normalized Difference Vegetation Index (NDVI) of 0.4. Accomplishing this requires that LightSAR (1) operate at L band or lower frequency—many experiments have shown that the estimated soil moisture for L-band frequencies correlate best with *in situ* measurements of soil moisture in the top 5 cm of the soil; (2) measure backscatter simultaneously at least at HH and VV polarizations (two measurements are required to separate the effects of surface roughness and soil moisture; full polarimetric capability is preferred but not required); (3) have a spatial resolution of 100 m or better to adequately sample the spatial variability in soil moisture; (4) have repeat observations of the same area at least every 8 days to adequately sample the temporal variability of soil moisture; and (5) repeat observations of the same area at as close to the same time of day as possible in order to minimize the effect of the diurnal variation in soil moisture on the measurement—predawn observations are preferred, but not required.

The redistribution of water is governed partly by atmospheric circulation. In recent years, models have been developed to trace circulation through space and time. Topographic roughness is a key parameter for such models, but one for which mapping data are mostly lacking. The ability to map large areas based on the radar backscatter coefficient was demonstrated by SIR-C for L band. The application of this technology to help refine circulation models will enable better understanding of water vapor transport, as well as general atmospheric motions.

### 2.4.2 Snow Properties: Snow Cover and Snow–Water Equivalence

Traditionally, satellite data have been used extensively to map snow-covered area—i.e., to determine whether a pixel is snow-covered or snow-free. In clear weather, optical sensors map the presence of snow best. A C-band dual-polarized SAR can map snow presence about 80% as well as the Landsat Thematic Mapper in all weather conditions, with the advantage that SAR can detect whether the snow is wet or dry. Snow cover data are incorporated into operational snowmelt forecasting schemes, but the size of a snow-covered area may not be a reliable indicator of the amount of water stored in the snowpack.

The most fundamental snow property in terms of water supply forecasting is the snow–water equivalence, which is the total amount of water the snow would yield at a point if it melted. Traditionally, this variable has been measured at several hundred snow courses throughout the mountainous regions of the western U.S. However, these snow courses do not adequately sample the terrain's variability—they are all on flat ground—and simple interpolation between snow courses does not produce useful results. Hence, the traditional snow course data provide only an index to the amount of water in a basin. They do not provide data that are accurate enough to calculate a water balance for the basin.

There is a need to estimate the spatial distribution of snow–water equivalence and its basin-wide integral. Experiments with SIR-C/X-SAR data show that direct measurement of snow–water

equivalence is now within our technological capability. The technique requires dual-polarization L-band data to estimate snow density, along with C-band data to estimate depth. The product of depth and density is the snow–water equivalence. Density does not vary rapidly, so the L-band and C-band measurements do not have to be simultaneous. Thus, C-band data from Radarsat or ERS/ENVISAT can supplement the LightSAR data acquisitions.

With accurate estimates of snow-covered area, detection of melting snow, and the measurement of the spatial distribution of snow–water equivalence, we will be able to better forecast melt on short and season-long time scales. Such forecasts will improve the management of reservoirs in areas of snowmelt runoff and thus improve the allocation of water for agriculture and other uses.

### ***2.5 The Role of the Ocean in Climate Change***

Synthetic aperture radar images of the oceans contain large amounts of information on both coastal and deep-ocean physical processes. This information is varied and impacts a rather wide variety of scientific oceanic disciplines. However, in the context of a global oceanic mission for LightSAR, probably the most significant is the role of the oceans in climate change. The importance of this role has been established by numerous publications and has led to major observational and theoretical programs. These research activities will continue well past the lifetime of LightSAR and thus will be significantly enhanced by the data provided by LightSAR.

The world's oceans play an exceedingly important role in establishing global weather and its long-term average, climate. The oceans have the only significant heat capacity on the surface of the Earth, because (a) water has the largest specific heat of any known substance (save one), and (b) the seas cover 71% of the surface of the planet. The land heats up and cools down on diurnal time scales, and the atmosphere is far too tenuous to store heat in any concentration. Thus, if significant amounts of solar energy are to be stored or released on time scales exceeding a few days, the oceans must be looked to for the mechanisms of retention and release; they are well-known to provide those mechanisms.

#### **2.5.1 Air–Sea Interaction and Ocean Climate Dynamics**

Synthetic aperture radar images have recently been shown to display signatures that discriminate important air–sea interaction processes due to sensitivity to small-scale surface roughness. Although the roughness modulations are often small (on the order of a few percent), they nevertheless are quite apparent in the imagery and often mirror significant and extensive dynamics. For example, it is the interaction between the planetary boundary layer of the atmosphere and the upper ocean that establishes the interchange of heat, momentum, and moisture in both the lower and upper atmospheric regions. It is those fluxes that must be determined if we are to understand the processes that control the mean temperature of the Earth, its humidity and cloudiness, and the amount of carbon dioxide in the atmosphere. Changes in long-term heat storage and release are major factors in the establishment of climate variability. While problems such as increases in carbon dioxide concentrations in the atmosphere are clearly important, it must be remembered that water vapor is a more radiatively active gas than carbon dioxide and is much more variable in time and space.

## LightSAR Science Requirements

Much, if not most of the air–sea interchange occurs episodically during storms and high wind events. During these events, the surface of the sea is hidden from remote sensors such as visible and infrared scanners because of cloud cover. Furthermore, ship- and buoy-based measurements are inhibited or even compromised during such heavy weather episodes. Thus, it is not presently possible to make accurate observations during those times when the physics is most active. It is at these times that spaceborne SAR provides views of the sea surface that are difficult to obtain by any other means.

The most important LightSAR requirements for oceanography are: (1) a wide swath—250 to 500 km—because the spatial scales of the important processes are well in excess of the so-called oceanic Rossby radius of deformation (typically 50 km at mid-latitudes); (2) dual polarization (HH and VV), because of the possibility of delineating atmospheric fluxes via differences in signatures in the two polarizations; and (3) repeated observations of the non-stationary processes at work, with a repeat time on the order of a week. Both open-ocean and coastal observations are desired, the latter because many important mechanisms go on near the edges of the continental shelves. Many features visible in SAR images of coastal regions also benefit fishing, boating, shipping, and offshore oil interests.

The climate-oriented observational program would likely concentrate on a few areas of the ocean known to be important: the Gulf Stream, the Greenland/Labrador Seas, the Norwegian Sea, and the Pacific equatorial current systems (this is an example of a tropical region). Observations would be focused on places and times when other relevant ocean research programs were taking place, thus leveraging the resources and providing “sea truth” to the SAR. The details of the observational strategy to be used by LightSAR will depend on these *in-situ* programs.

### **3. LightSAR Sensor Requirements**

Figure 1 shows the traceability from the LightSAR science objectives to sensor requirements.

#### **3.1 *Frequency***

An L-band sensor is required for repeat-pass interferometry and surface characterization.

Traceability: Crustal Deformation 2.1.1; Volcanology 2.1.2; Glaciology 2.2.1; Forest Regrowth 2.3.1; Soil Moisture 2.4.1; Snow Density 2.4.2.

#### **3.2 *Change Detection***

The mission shall include a mode of operation that will allow a 110-km-wide strip of L-band HH image data to be acquired continuously at a resolution of at least 25 meters and a phase accuracy allowing a surface displacement resolution of 2-5 mm statistical height error over any swath. Any ground location shall be visible every 8-10 days, and all ground locations shall be visible every 24 days, with a minimum incidence angle of 20°.

Traceability: Crustal Deformation 2.1.1; Volcanology 2.1.2; Glaciology 2.2.1.

#### **3.3 *Multi-incidence-angle Observations***

The mission shall include modes of operation that will allow observations ranging from 20° to 45° from nadir.

Traceability: Required for rapid site revisit capability for earthquake and volcano deformation studies. Crustal Deformation 2.1.1; Volcanology 2.1.2.

#### **3.4 *Polarimetric Observations***

The mission shall include a mode of operation that will allow the simultaneous acquisition of the four polarization combinations: HH, HV, VH, and VV. This mode shall have a spatial resolution of at least 25 m and a continuous swath of at least 50 km.

Traceability: Forest Regrowth and Biomass 2.4.1; Soil Moisture 2.4.1; Snow Density 2.4.2.

#### **3.5 *Wide-swath/Dual-polarization Mode***

The mission shall include a mode of operation that will allow a 250-500 km swath to be imaged continuously with a spatial resolution of at least 100 m. This mode must be a dual-polarization (HH/VV) mode.

Traceability: Ocean Feature and Mesoscale Eddy Mapping 2.5.1.

## **4. LightSAR Orbital Requirements**

### **4.1 *Inclination***

The ability to image both poles is required.

Traceability: Ice.Sheet Mass Balance and Sea Level Objectives 2.2

### **4.2 *Repeat/Revisit Period***

The revisit (exact repeat) time shall be 8-10 days.

Traceability: Crustal Deformation 2.1.1; Volcanology 2.1.2; Glaciology Objectives 2.2.1.

### **4.3 *Orbital Control***

Sufficient orbital control is required to guarantee interferometric baselines less than 250 m.

Traceability: Crustal Deformation 2.1.1; Volcanology 2.1.2; Glaciology Objectives 2.2.1.

### **4.4 *Orbital Knowledge***

< 10 cm orbit knowledge within one orbit is required.

Traceability: Crustal Deformation 2.1.1; Volcanology 2.1.2; Glaciology Objectives 2.2.1.

## **5. LightSAR Operational Requirements**

### **5.1 *Mission Duration***

The LightSAR mission shall be designed for a 60-month (5-year) duration, equal to the planned life of the spacecraft.

Traceability: Crustal Deformation 2.1.1; Volcanology 2.1.2; Glaciology Objectives 2.2.1.

### **5.2 *Data Volume and Rate***

The LightSAR mission shall collect at least 6 minutes of interferometry data per orbit on average (see Figure 2), with 16 minutes being the peak. In addition, the LightSAR mission shall collect at least 1.5 minutes per orbit of fully polarimetric and/or dual-polarized data to meet the science objectives for monitoring forest regrowth and soil moisture.

Traceability: Crustal Deformation 2.1.1; Volcanology 2.1.2; Glaciology Objectives 2.2.1; Forest Regrowth and Biomass 2.3.1; Soil Moisture 2.4.1.

### **5.3 *Real-time Mission Planning***

Updates to the nominal timeline will require approval by a Mission Planning Board. Requests for new acquisitions to catch transient events will need to be accommodated.

Traceability: Crustal Deformation 2.1.1; Volcanology 2.1.

## **6. Mode-Specific Requirements**

### **6.1 *Radiometric Accuracy and Precision***

Relative amplitude calibration of 1 dB is required

Traceability: Forest Regrowth and Biomass 2.4.1; Soil Moisture 2.4.1; Snow Density 2.4.2.

### **6.2 *Phase Accuracy and Precision***

Phase calibration  $10^\circ$ .

Traceability: Forest Regrowth and Biomass 2.4.1; Soil Moisture 2.4.1; Snow Density 2.4.2.

### **6.3 *Channel-to-channel Amplitude Calibration***

Channel-to-channel amplitude calibration of .5 dB is required.

Traceability: Forest Regrowth and Biomass 2.4.1; Soil Moisture 2.4.1; Snow Density 2.4.2.

### **6.4 *Polarization Isolation***

A polarization isolation of -25 dB is required.

Traceability: Forest Regrowth and Biomass 2.4.1; Soil Moisture 2.4.1; Snow Density 2.4.2.

### **6.5 *Noise-equivalent $S_0$***

A noise-equivalent  $\sigma_0$  of -30 dB is required across the swath.

Traceability: Crustal Deformation 2.1.1; Volcanology 2.1.

## 7. Recommended Mission Enhancements

### 7.1 *Direct-broadcast Capability at X Band*

### 7.2 *Added Frequency (C or X Band)*

The sensor parameters given in Section 3 are the minimum set utilizing a single frequency to meet the most essential science requirements described under Section 2, *Science Objectives*. These parameters do not, by any means, define the complete set of measurement requirements to achieve the radar-related goals for each of the science disciplines. For example, as shown in Table 2, a number of science applications require C-band, X-band, or P-band frequencies. Due to the narrower scope of applications and the degree of maturity of sensor design issues, the P-band frequency is not recommended as a mission enhancement for LightSAR. However, the C-band (and to a smaller degree the X-band) frequency is expected to provide higher-return additions to LightSAR's L-band sensor. Due to broader availability of C-band spaceborne sensors to date, several applications have been demonstrated and validated with C band, and some are in the operations phase.

The addition of a C-band SAR will enhance the following science objectives:

- Ice sheet velocity (2.2.1)—C band interferometric mode with shorter repeat cycle
- Glacier volume and topography (2.2.2, 2.2.3)—C band interferometric mode with shorter repeat cycle
- Vegetation water content (2.3, 2.4)—C band dual-polarization.

The addition of a C-band (or X-band) SAR will enable the following science areas:

- Snow extent and wetness (2.4.2)—C band quad-polarization
- Snow depth (2.4.2)—C band or X band HH or VV
- Inundation in nonwoody wetlands (2.1.3,2.4)—C band HH or VV
- Ocean ice motion (2.5)—C band interferometric mode with shorter repeat cycle.

## 8. Acknowledgement

This work was performed in part by the Jet Propulsion Laboratory, California Institute of Technology, under contract with the National Aeronautics and Space Administration.

# LightSAR Science Requirements

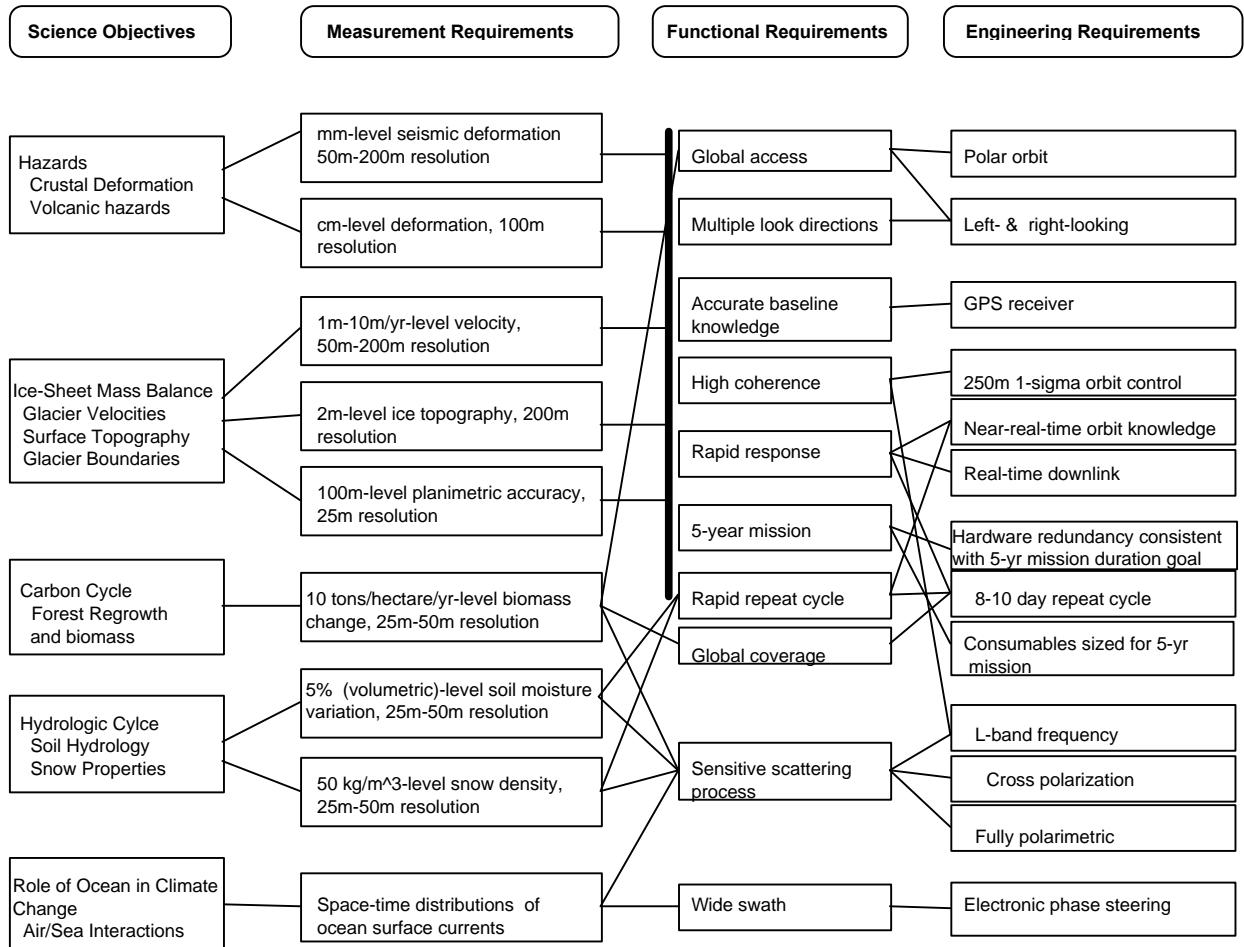
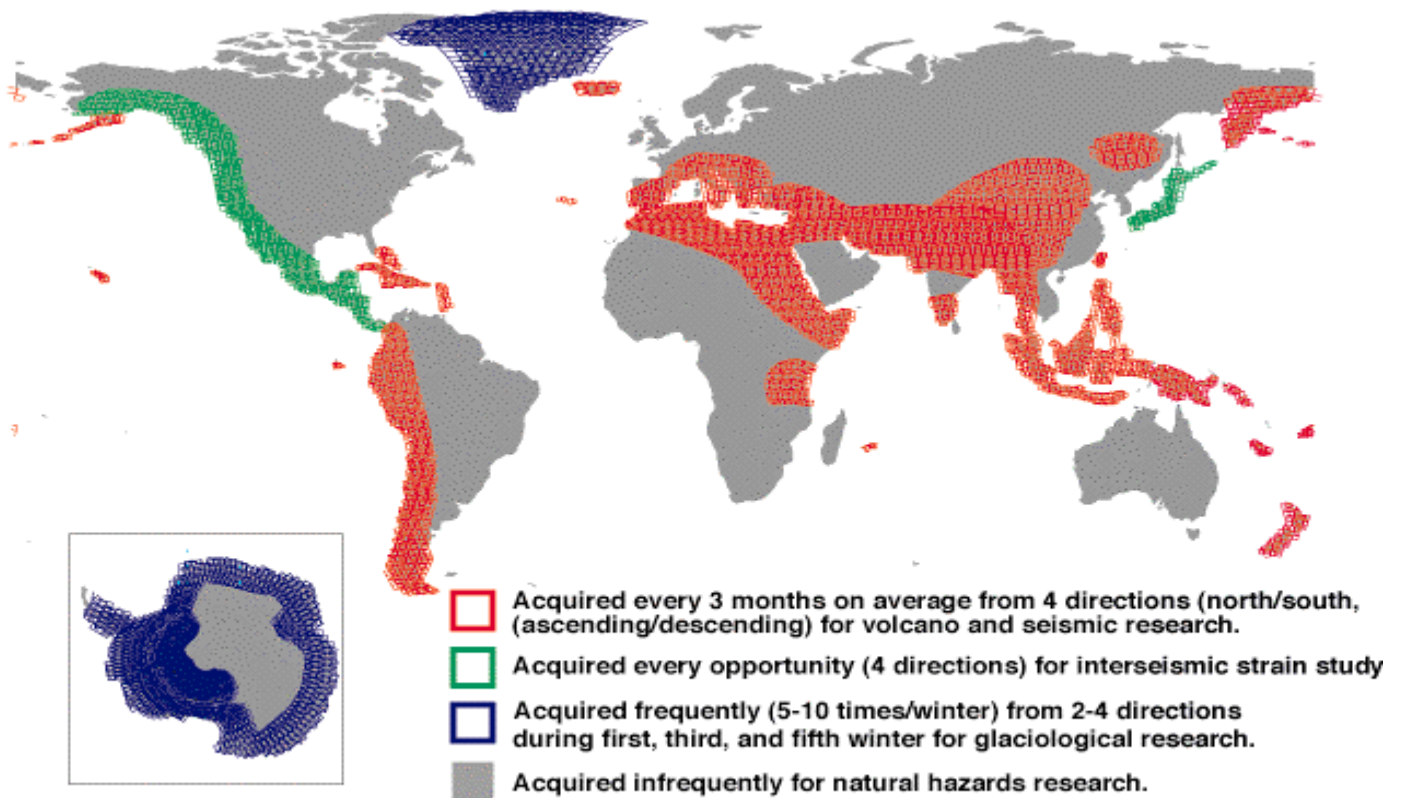


**Figure 1. Flow from Science Objectives to Requirements**



This coverage requires an average of 5.85 min/orbit (16 min peak/orbit) over the 5 year mission

Figure 2. Sample Coverage Requirements for Interferometry

# LightSAR Science Requirements

**Table 1. Current and Planned SAR Systems**

| PARAMETER                     | ERS-1        | ERS-2         | SIR-C               | X-SAR<br>(flown with SIR-C) | RADARAT                     | ENVISAT<br>(ASAR) | JERS-1           | PALSAR               | MIR-<br>PRIRODA | ALMAZ-1       | MITI SAR-2 |
|-------------------------------|--------------|---------------|---------------------|-----------------------------|-----------------------------|-------------------|------------------|----------------------|-----------------|---------------|------------|
| RADAR BAND                    | C            | C             | C,L                 | X                           | C                           | C                 | L                | L                    | L,S             | S             | L          |
| POLARIZATION                  | VV           | VV            | ALL                 | VV                          | HH                          | HH/VV/HV          | HH               | HH or VV<br>HV or VH | *               | HH            | HH         |
| INCIDENCE<br>ANGLE (°)        | 24           | 24            | 17-60               | 17-60                       | 17-50                       | 20-45             | 35               | 20-55                | 35              | 30-60         | 20-45      |
| RESOLUTION (m)                | 25           | 25            | 25                  | 25                          | 10-100                      | 30                | 18               | 10-100               | *               | 15            | 10-100     |
| SWATH WIDTH (km)              | 100          | 100           | 15-100              | 15-40                       | 50-170<br>(5 km in ScanSAR) | 50-400            | 76               | 70-250               | 120             | 20-45         | 50-500     |
| SYSTEM<br>SENSITIVITY (dB)    | -25          | -25           | -50                 | -22                         | -23                         | *                 | -20              | -25                  | *               | *             | -25        |
| ALTITUDE (km)                 | 790          | 785           | 225                 | 225                         | 790                         | 800               | 568              | 700                  | 394             | 300           | 700        |
| SIMULTANEOUS<br>FREQUENCIES   | 1            | 1             | 3                   | 3                           | 1                           | 1                 | 1                | 1                    | 2               | 1             | 1          |
| SIMULTANEOUS<br>POLARIZATIONS | 1            | 1             | 4                   | 4                           | 1                           | 2                 | 1                | 2                    | *               | 1             | 1          |
| ORBIT<br>INCLINATION (°)      | 97.7         | 97.7          | 57                  | 57                          | 98.6                        | 100               | 97.7             | 98                   | 51.6            | 72.7          | 97.7       |
| BANDWIDTH (MHz)               | 13.5         | 13.5          | 10,20               | 10,20                       | 12-30                       | 14                | 15               | 30                   | *               | *             | 50         |
| DATA RATE (Mbps)              | 165          | 165           | 90 or<br>46/channel | 45                          | 110                         | 100               | 60               | 240                  | *               | *             | 240        |
| LAUNCH DATE                   | July<br>1991 | April<br>1995 | April/Oct<br>1994   | April/Oct<br>1994           | fall<br>1995                | late<br>1998      | February<br>1992 | August<br>2002       | 1995            | March<br>1991 | 2001       |
| LIFETIME (years)              | 3            | 3             | 11 DAYS             | 11DAYS                      | 5                           | 5                 | 2<br>minimum     | 3-5                  | 2               | 2.5           | 3-5        |

## LightSAR Science Requirements

**Table 2. Examples of SAR Applications**

| Geophysical parameters                              | Algorithms and mission parameters   | Maturity (i.e. readiness for operational use)   |
|---|---|---|
| Surface deformation                                 | Repeat-pass interferometry within 1 month; L band; orbit control  | Validated (line-of-sight) Demonstrated (vector) |
| <i>Pre-seismic</i>                                  | Multiple repeats (noise identification & reduction)   | Research  |
| <i>Co-seismic</i>                                   | Pre- and post- coverage   | Validated                                       |
| <i>Post-seismic</i>                                 | Targeted coverage   | Validated                                       |
| <i>Inter-seismic</i>                                | Extended regional areal coverage (100s km) at low-resolution (25 m); long time series (yr), regular repeats (mo). | Demonstrated (creep zones)                      |
| <i>Pre-eruptive</i>                                 | Multiple repeats (noise identification and reduction)   | Research (other areas)                          |
| <i>Co-eruptive</i>                                  | Targeted coverage   | Research  |
| <i>Inter-eruptive</i>                               | Long time series. Regular repeats.  | Validated                                       |
| <i>Landslides</i>                                   | Local coverage, high resolution.  | Demonstrated                                    |
| <i>Subsidence</i>                                   | Regional & local coverage   | Demonstrated                                    |
| Other geometrical surface changes (e.g., lava flow) | Long time series; Regular repeats; L band   | Demonstrated                                    |
| Glacier & ice sheet velocity                        | <i>Ice sheets</i> L Band repeat-pass interferometry within 8 days, or C band within 2 days, at latitude > 65°     | Demonstrated (L-band)                           |
|   | <i>Glaciers</i> Repeat-pass interferometry (1-2 days?) or pattern matching  | Validated (C-band)                              |
| Glacier volume & topography                         | L Band repeat-pass interferometry within 8 days, or C band within 2 days  | Demonstrated                                    |
| Forest biomass                                      | <i>Boreal</i> L band HV   | Demonstrated                                    |
|   | <i>Temperate</i> L band HV or P band HV   | Demonstrated                                    |
|   | <i>Tropical</i> P band HV   | Demonstrated                                    |
| Vegetation Classification                           | <i>Forest</i> L band dual pol.  | Research  |
|   | <i>Crops</i> L band quad pol.   | Research  |
| Aerodynamic roughness                               | L band HV   | Demonstrated                                    |
| Vegetation Moisture                                 | L dual pol., or C dual pol. (+ species type ancillary)  | Research  |
| Soil moisture                                       | <i>Bare</i> L band quad-pol.  | Demonstrated                                    |
|   | <i>Grass and shrubs</i> L band quad-pol.  | Research  |
|   | <i>Forest</i> P band quad-pol.  | Research (early research?)                      |
| Snow volume and extent                              | <i>Snow-covered area</i> C band HH + DEM, or C band quad-pol.   | Demonstrated                                    |
|   | <i>Wetness</i> C band quad-pol.   | Research  |
|   | <i>Water equivalence</i> Density from L -Quad pol. + depth from C or X-band                                       | Research  |
| Inundation and extent (floods)                      | <i>Forests</i> L band HH  | Demonstrated                                    |
|   | <i>Non-woody wetlands</i> C band HH or VV   | Demonstrated                                    |
| Post flood inventory                                | C and L band HH and HV  | Demonstrated                                    |
| Oceans  | <i>Ice motion</i> C band HH and 3-day repeat  | Operational                                     |
|   | <i>Ice type</i> L band quad-pol.  | Demonstrated                                    |
|   | <i>Mesoscale circulation</i> L band quad-pol.   | Research  |

## Appendix A: LightSAR Science Working Group (LSWG) Members

Dr. John Apel  
Global Ocean Associates  
P.O. Box 12131  
Silver Spring, MD 20908-2131  
globocen@erols.com

Dr. Raymond Arvidson  
Washington University  
Department of Earth and  
Planetary Sciences  
St. Louis, MO 63031  
arvidson@wunder.wustl.edu

Dr. Miriam Baltuck  
Code YS  
NASA HQ  
Washington, DC  
mbaltuck@hq.nasa.gov

Dr. Robert Bindschadler  
NASA-GSFC  
Code 971, Building 17, Room  
N206  
Greenbelt Road  
Greenbelt, MD 20771  
bob@igloo.gsfc.nasa.gov

Dr. Frank Carsey  
Jet Propulsion Laboratory  
Mail Stop 300-323  
4800 Oak Grove  
Pasadena, CA 91109  
frank.carsey@jpl.nasa.gov

Dr. Timothy Dixon  
RSMAS  
4600 Rickenbacker Causeway  
Miami, FL 33149  
tim@corsica.rsmas.miami.edu

Dr. Jeff Dozier  
University of California  
(UCSB)  
School of Environmental  
Science and Management  
Santa Barbara, CA 93106  
dozier@crseo.ucsb.edu

Dr. Diane Evans

Jet Propulsion Laboratory  
Mail Stop 180-703  
4800 Oak Grove Drive  
Pasadena, CA 91109  
devans@jpl.nasa.gov

Dr. Oscar Karl Huh  
Earth Scan Lab of the Coastal  
Studies Institute  
Louisiana State University  
Baton Rouge, Louisiana 70803  
oscar@antares.esl.lsu.edu

Dr. Kenneth Jezek  
Byrd Polar Research Center  
108 Scott Hall  
1090 Carmack Rd.  
Columbus, OH 43210  
jezek@iceberg.mps.ohio-  
state.edu

Dr. Eric Kasischke  
ERIM  
P.O. Box 134001  
Ann Arbor, MI 48113-4001  
ekas@erim.org

Dr. Fuk Li  
Jet Propulsion Laboratory  
Mail Stop 300-331  
4800 Oak Grove Drive  
Pasadena, CA 91109  
fuk.li@jpl.nasa.gov

Dr. John Melack  
University of California  
(UCSB)  
Department of Biological  
Sciences  
Santa Barbara, CA 93106  
melack@artemia.ucsb.edu

Dr. Jean-Bernard Minster  
Scripps Institute of  
Oceanography  
University of San Diego  
9500 Gilman Drive  
La Jolla, CA 92093  
jbminster@ucsd.edu

Dr. Peter Mouginiis-Mark  
University of Hawaii  
Hawaii Institute of Geophysics  
and Planetology  
2525 Correa Road  
Honolulu, Hawaii 96822  
pmm@kahana.pgd.hawaii.edu

Dr. Earnest D. Paylor, II  
Geology Program Scientist  
NASA Headquarters  
300 E. St. SW  
Washington, DC 20546

Dr. Paul Rosen  
Jet Propulsion Laboratory  
Mail Stop 300-235  
4800 Oak Grove Drive  
Pasadena, CA 91109  
Paul.A.Rosen@jpl.nasa.gov

Dr. Jakob van Zyl  
NASA Jet Propulsion  
Laboratory  
Mail Stop 300-227  
4800 Oak Grove Drive  
Pasadena, CA 91109  
jacobv@kalfie.Jpl.Nasa.Gov

Dr. Howard Zebker  
Department of Electrical  
Engineering  
232 Durand, STARLAB  
Stanford University  
Stanford CA, 94305-9515  
zebker@jakey.stanford.edu

**Appendix B: Additional Science Contacts**

Dr. Anthony Freeman (Radar System Engineering)

JPL

freeman@ampersand.jpl.nasa.gov

Dr. Ian Joughin (Ice-sheet Mass Balance and Sea Level)

JPL

Ian.R.Joughin@jpl.nasa.gov

Dr. Mahta Moghaddam (Radar Science)

JPL

mahta@ampersand.jpl.nasa.gov

Dr. Sasan Saatchi (Vegetation Studies)

JPL

Sasan.S.Saatchi@jpl.nasa.gov

## Appendix C: References

1. Abdelsalam, M., and R. Stern, "Mapping Precambrian structures in the Sahara Desert with SIR-C/X-SAR radar: The Neoproterozoic Keraf Suture, NE Sudan," *J. Geophys. Res.*, vol. 101, no. E10, pp. 23063-23076, 1996.
2. Anys, H., and D. He, "Evaluation of textural and multipolarization radar features for crop classification," *IEEE Trans. Geosci. Remote Sensing*, vol. 33, no. 5, pp. 1170-1181, 1995.
3. Apel, J., "An improved model of the ocean surface wave vector spectrum and its effects on radar backscatter," *J. Geophys. Res.*, vol. 99, no. CB, pp. 16269-16291, 1994.
4. Beal, R., D. Tilley, and F. Monaldo, "Large and small scale spatial evolution of digitally processed ocean wave spectra from Seasat synthetic aperture radar," *J. Geophys. Res.*, vol. 88, pp. 1761-1778, 1983.
5. Beaudoin, A., et al., "Retrieval of forest biomass from SAR data," *Int. J. Remote Sensing*, vol. 15, pp. 2777-2796, 1994.
6. Carsey, F., and R. Garwood, "Identification of modeled ocean plumes in Greenland gyre ERS-1 SAR data," *Geophys. Res. Lett.*, vol. 20, pp. 2207-2210, 1993.
7. De Grandi, G., G. de Groof, C. Lavallo, A. Sieber, "Fully polarimetric classification of the Black Forest MAESTRO 1 AIRSAR data," *Int. J. Remote Sensing*, vol. 15, pp. 2755-2775, 1994. (P band)
8. Dixon, T. H., Ed., *SAR Interferometry and Surface Change Detection*, Report of a workshop held in Boulder, Colorado, University of Miami Rosenstiel School of Marine and Atmospheric Science, RSMAS Technical Report TR 95-003, 1995.
9. Dobson, M. C., et al., "Estimation of forest biomass characteristics in Northern Michigan with SIR-C/X-SAR data," *IEEE Trans. Geosci. Remote Sensing*, vol. 33, pp. 877-894.
10. Drinkwater, M., et al., "Potential applications of polarimetry to the classification of sea ice," in *Microwave Remote Sensing of Sea Ice*, F. Carsey, Ed., Geophysical Monograph 68, AGU, Washington, D.C., pp. 419-430, 1992.
11. Dubois, P., J. van Zyl, and T. Engman, "Measuring soil moisture with imaging radars," *IEEE Trans. Geosci. Remote Sensing*, vol. 33, no. 4, pp. 915-926, 1995.
12. Evans, D., et al., *Spaceborne Synthetic Aperture Radar: Current Status and Future Directions*, NASA Technical Memorandum 4679, 171 pgs., 1995.
13. Fetterer, F., D. Gineris, and R. Kwok, "Sea-ice type maps from Alaska Synthetic Aperture Radar Facility imagery: An assessment of Arctic multiyear ice coverage estimated through Alaska SAR Facility data analysis," *J. Geophys. Res.* vol. 99, no. C11, pp. 22443-22458, 1994.
14. Foody, G., M. McCulloch, and W. Yates, "Crop classification from C-band polarimetric radar data," *Int. J. Remote Sensing*, vol. 15, pp. 2871-2885, 1994.
15. Forget, P., and Pierre Broche, "Slicks, waves, and fronts observed in a sea coastal area by an X-band airborne," *Remote Sensing Environ.*, vol. 57, no.1, pp. 1-12, 1996.
16. Freeman, A., and S. Durden, "A three-component scattering model for polarimetric SAR data," *IEEE Trans. Geosci. Remote Sensing*, submitted, 1996.
17. Gabriel, A. G., R. M. Goldstein, and H. A. Zebker, "Mapping small elevation changes over large areas: Differential radar interferometry," *J. Geophys. Res.*, vol. 94, pp. 9183-9191, 1989.
18. Goldstein, R. M., H. A. Zebker, C. L. Werner, "Satellite radar interferometry: Two-dimensional phase unwrapping," *Rad. Sci.*, vol. 23, pp. 713-720, 1988.
19. Goldstein, R. M., H. Engelhardt, B. Kamb, and R. M. Frolich, "Satellite radar interferometry for monitoring ice sheet motion: Application to an Antarctic ice stream," *Science*, vol. 262, pp. 1525-1530, 1993.
20. Goldstein, R. M., "Atmospheric limitations to repeat-track radar interferometry," *Geophys. Res. Lett.*, vol. 22, pp. 2517-2520, 1995.
21. Greeley, R., and D. Blumberg, "Preliminary analysis of Shuttle Radar Laboratory (SRL-1) data to study," *IEEE Trans. Geosci. Remote Sensing*, vol. 33, no. 4, pp. 927-933, 1995.
22. Harrell, P., E. Kasischke, L. Borgeau-Chavez, E. Haney, and N. Christensen, Jr., "Evaluation of approaches to estimate above-ground biomass in Southern pine forests using SIR-C data," *Remote Sensing Environ.*, in press.
23. Hartl, Ph., K. H. Thiel, X. Wu, Ch. Doake, and J. Sievers, "Application of SAR interferometry with ERS-1 in the Antarctic," *Earth Observation Quarterly*, no. 43, pp. 1-4, 1995.
24. Hess, L., J. Melack, S. Filoso, and Y. Wang, "Delineation of inundated area and vegetation along the Amazon floodplain with the SIR-C synthetic aperture radar," *IEEE Trans. Geosci. Remote Sensing*, vol. 33, no. 4, pp. 896-904, 1995.

## LightSAR Science Requirements

25. Holt, B., A. Rothrock, and R. Kwok, "Determination of sea ice motion from satellite images," in *Microwave Remote Sensing of Sea Ice*, F. Carsey, Ed., Geophysical Monograph 68, pp. 344-354, AGU, Washington, D.C., 1992.
26. Izenberg, N.R., R.E. Arvidson, R.A. Brackett, S.S. Saatchi, G.R. Osburn, and J. Dohrenwend, "Erosional and depositional patterns associated with the 1993 Missouri River floods inferred from SIR-C and TOPSAR radar data," *J. Geophys. Res.*, vol. 101, pp. 23,149-23,168, 1996.
27. Joughin, I., D. P. Winebrenner, and M. A. Fahnestock, "Observations of ice-sheet motion in Greenland using satellite radar interferometry," *Geophys. Res. Lett.*, vol. 22, no. 5, pp. 571-574, 1995.
28. Joughin, I., D. Winebrenner, M. Fahnestock, R. Kwok, and, W. Krabill, 1996, "Measurement of ice-sheet topography using satellite radar interferometry," *J. Glaciology*, vol. 42, no. 140, 1996.
29. Joughin, I., R. Kwok, M. Fahnestock, "Estimation of ice sheet motion using satellite radar interferometry: method and error analysis with application to the Humboldt Glacier, Greenland," *Journal of Glaciology*, in press.
30. Joughin, I., S. Tulaczyk, M. Fahnestock, R. Kwok, "A mini-surge on the Ryder Glacier, Greenland observed via satellite radar interferometry," *Science*, vol. 274, pp. 228-230, 1996.
31. Kasischke, E., N. Christensen, and L. Borgeau-Chavez, "Correlating Radar backscatter with components of *IEEE Trans. Geosci. Remote Sensing*, vol. 33, no. 3, pp. 643-659, 1995.
32. Kasischke, E., J. Melack, and M. C. Dobson, "The use of imaging radars for ecological applications - A review," *Remote Sensing Environ.*, in press.
33. Kwok, R., E. Rignot, B. Holt, and R. Onstott, "Identification of sea ice types in spaceborne synthetic aperture radar," *J. Geophys. Res.*, vol. 97, no. C2, pp. 2391-2402, 1992.
34. Kwok, R., E. Rignot, J. Way, A. Freeman, and B. Holt, "Polarization signatures of frozen and thawed forests of *IEEE Trans. Geosci. Remote Sensing*, vol. 32, pp. 371-381, 1994.
35. Kwok, R., M. A. Fahnestock, "Ice sheet motion and topography from radar interferometry," *IEEE Trans. Geosci. Rem. Sen.*, vol. 34, no. 1, 1996.
36. Le Toan, T., A. Beaudoin, J. Riou, and D. Guyon, "Relating forest biomass to SAR data," *IEEE Trans. Geosci. Remote Sensing*, vol. 30, no. 2, pp. 403-411, 1992.
37. Liu, A., C. Peng, and J. Schumacher, "Wave-current interaction study in the Gulf of Alaska for the detection of *J. Geophys. Res.*, vol. 99, pp. 10075-10085, 1994.
38. Massonnet, D. and K. Fiegl, "Satellite radar interferometric map of the co-seismic deformation field of the M=6.1 Eureka Valley, CA earthquake of May 17, 1993," *Geophys. Res. Lett.*, vol. 22, pp. 541-1544, 1995.
39. Massonnet, D., P. Briole, and A. Arnaud, "Deflation of Mount Etna monitored by spaceborne radar interferometry," *Nature*, vol. 375, pp. 567-570, 1995.
40. Moghaddam, M., S. Durden, and H. Zebker, "Radar measurements of forested areas during OTTER," *Remote Sensing Environ.*, vol. 47, pp. 154-166, 1994.
41. Moghaddam, M., and S. Saatchi, "Analysis of scattering mechanisms in SAR imagery over boreal forest: Results *IEEE Trans. Geosci. Remote Sensing*, vol. 33, no. 5, pp. 1290-1296, 1995.
42. Moghaddam, M., and S. Saatchi, "Monitoring tree moisture using an inversion algorithm applied to SAR data *IEEE Trans. Geosci. Remote Sensing*, submitted, 1996.
43. Monaldo, F., and R. Beal, "Tral-time observations of Southern Ocean wave fields from the Shuttle Imaging *IEEE Trans. Geosci. Remote Sensing*, vol. 33, no. 4, pp. 942-949, 1995.
44. Onstatt, R., "SAR and scatterometer signatures of sea ice," in *Microwave Remote Sensing of Sea Ice*, F. Carsey, Ed., Geophysical Monograph 68, AGU, Washington, D.C., 1992.
45. Peltzer, G., P. A. Rosen, "Surface displacement of the 17 May 1993 Eureka Valley, California, earthquake observed by SAR interferometry," *Science*, vol. 268, p. 1333, 1995.
46. Pope, K., E. Rejmankova, J. Paris, and R. Woodruff, "Monitoring seasonal flooding cycles in marshes of the Yucatan Peninsula with SIR-C polarimetric radar imagery," *Remote Sensing Environ.*, in press.
47. Pope, K., J. Rey-Benayas, and J. Paris, "Radar remote sensing of forest and wetland ecosystems in the Central American tropics," *Remote Sensing Environ.*, vol. 48, pp. 205-219, 1994.
48. Pope, K., et al., "Identification of central Kenyan Rift Valley fever virus vector habitats with Landsat TM and evaluation of their flooding status with airborne imaging radar," *Remote Sensing Environ.*, vol. 40, pp. 185-196, 1992.
49. Ranson, J., and G. Sun, "Northern forest classification using temporal multifrequency and multipolarimetric SAR images," *Remote Sensing Environ.*, vol. 47, pp. 142-153, 1994.

## LightSAR Science Requirements

50. Ranson, J., S. Saatchi, and G. Sun, "Boreal forest ecosystem characterization with SIR-C/X-SAR," *IEEE Trans. Geosci. Remote Sensing*, vol. 33, no. 4, pp. 867-876, 1995.
51. Ranson, J., and G. Sun, "Mapping biomass of a northern forest using multifrequency SAR data," *IEEE Trans. Geosci. Remote Sensing*, vol. 32, no. 2, pp. 388-396, 1995.
52. Rignot, E., J. B. Way, "Monitoring freeze-thaw cycles along north-south Alaskan transects using ERS-1 SAR," *Remote Sensing Environ.*, vol. 49, pp. 131-137, 1994.
53. Rignot, E., W. Salas, and D. Skole, "Mapping of deforestation and secondary growth in Rondonia, Brazil, using imaging Radar and thematic mapper data," *Remote Sensing Environ.*, in press.
54. Rignot, E., R. Zimmermann, J. van Zyl, and R. Oren, "Spaceborne applications of a P-band imaging radar for mapping of forest biomass," *IEEE Trans. Geosci. Remote Sensing*, vol. 33, no. 5, pp. 1162-1169, 1995.
55. Rignot, E., K. C. Jezek, and H. G. Sohn, "Ice flow dynamics of the Greenland ice sheet from SAR interferometry," *Geophys. Res. Lett.*, vol. 22, no. 5, pp. 575-578, 1995.
56. Rignot, E., "Tidal flexure, ice velocities, and ablation rates of Petermann Gletscher, Greenland," submitted to *J. Glaciology*, March 12, 1996.
57. Rignot, E., R. Forster, and B. Isacks, "Radar interferometric observations of Glacier San Rafael, Chile," *J. Glaciology*, vol. 42, no. 141, 1996. *Sci.*, vol. 31, no. 6, pp. 1449-1485, 1996.
58. Rosen, P., S. Hensley, H. Zebker, and F. Webb, "Surface deformation and coherence measurements of Kilauea volcano, Hawaii, from SIR-C radar interferometry," *J. Geophys. Res.*, vol. 101, no. E10, pp. 23109-23125, 1996.
59. Rott, H., T. Nagler, and D. Floricioiu, "Snow and glacier parameters derived from single channel and multiparameter SAR," Proc. Symposium on Retrieval of Bio- and Geophysical Parameters from SAR Data for Land Applications, Toulouse, France, pp. 479-488, 1995.
60. Saatchi, S., J. van Zyl, and G. Asrar, "Estimation of canopy water content in Konza Prairie grasslands using SAR" *J. Geophys. Res.*, vol. 100, no. D12, pp. 25481-25496, 1995.
61. Saatchi, S., J. V. Soares, and D. S. Alves, "Mapping deforestation and land use in Amazon rainforest using SIR-C imagery," *Remote Sensing Environ.*, vol. 59, 1997.
62. Schmullius, Ch., and D. Evans, "Synthetic aperture frequency and polarimetric requirements for applications in ecology, geology, hydrology, and oceanography - a tabular status quo after SIR-C/X-SAR," *Remote Sensing Environ.*, in press.
63. Shi, J., and J. Dozier, "Inferring snow wetness using C-band data from SIR-C's polarimetric synthetic aperture" *IEEE Trans. Geosci. Remote Sensing*, vol. 33, no. 4, pp. 905-914, 1995.
64. Shi, J., J. Dozier, and H. Rott, "Snow mapping in alpine regions with synthetic aperture radar," *IEEE Transactions on Geoscience and Remote Sensing*, vol. 32, no. 1, pp. 152-158, 1994.
65. Shi, J., and J. Dozier, "Estimation of snow-water equivalence using SIR-C/X-SAR," Proceedings IGARSS '96, IEEE 96CH35875, pp. 2002-2004, 1996.
66. Stern, H., D. Rothrock, and R. Kwok, "Open water production in the Arctic Sea ice cover: Satellite" *J. Geophys. Res.*, 1994.
67. Taylor, J., et al., "Characterization of saline soils using airborne Radar imagery," submitted, 1996.
68. Thompson, D., H. Graber, and R. Carande, "Measurements of ocean currents with SAR interferometry and HF
69. Treuhaft, R., S. Madsen, M. Moghaddam, and J. van Zyl, "Vegetation characteristics and underlying topography" *Rad. Sci.*, vol. 31, no. 6, pp. 1449-1485, 1996.
70. Van Zyl, J., "Unsupervised classification of scattering behavior using radar polarimetry data," *IEEE Trans. Geosci. Remote Sensing*, vol. 27, pp. 36-45, 1989.
71. Wang, J., A. Hsu, J. Shi, P. O'Neil, and T. Engman, "A comparison of soil moisture models using SIR-C measurements over the Little Washita River watershed," *Remote Sensing Environ.*, in press.
72. Wang, Y., L. Hess, S. Filoso, and J. Melack, "Canopy penetration studies: modeled radar backscatter from Amazon floodplain forests at C, L, and P band," *Remote Sensing Environ.*, vol. 55, pp. 324-332, 1995.
73. Zebker, H. A., P. A. Rosen, R. M. Goldstein, A. Gabriel, C. L. Werner, "On the derivation of co-seismic displacement fields using differential radar interferometry: The Landers earthquake," *J. Geophys. Res.*, vol. 99, p. 19617, 1994.
74. Zebker, H. A., P. A. Rosen, S. Hensley, P. J. Mouganis-Mark, "Analysis of active lava flows on Kilauea Volcano, Hawaii, using SIR-C radar correlation measurements," *Geology*, vol. 24, p. 495, 1995.